J Fluoresc (2008) 18:269–276
DOI 10.1007/s10895-007-0258-1

ORIGINAL PAPER

Photocharacterization of Novel Ruthenium Dyes and Their Utilities as Oxygen Sensing Materials in Presence of Perfluorochemicals

Ozlem Oter · Kadriye Ertekin · Osman Dayan · Bekir Cetinkaya

Received: 1 April 2005 / Accepted: 4 September 2007 / Published online: 12 October 2007

Abstract Photophysical constants of three novel ruthenium dyes derived from tridentate pyridinediimine (pydim) ligands has been declared and their photoluminescent properties were investigated in solvents of dichloromethane (DCM), tetrahydrofuran (THF) and ethanol (EtOH) by UV-Visible absorption, emission and excitation spectra. The quantum yield, fluorescence decay time, molar extinction coefficient and Stoke's shift values of the novel ruthenium complexes were determined. The perfluoro compound (PFC) nonadecafluorodecanoic acid which is also known as medical gas carrier has been used for the first time together with newly synthesized Ruthenium complexes in ethyl alcohol. The utilities of oxygen sensing materials were investigated in EtOH in presence of chemically and biochemically inert PFC.

Keywords Perfluorochemicals (PFCs) · Ruthenium complex · Quantum yield · Fluorescence spectroscopy · Optical oxygen sensing

O. Oter · K. Ertekin
Faculty of Arts and Sciences, Department of Chemistry,
University of Dokuz Eylul,
Tinaztepe,
35160 Izmir, Turkey

O. Dayan · B. Cetinkaya
Faculty of Science, Department of Chemistry, University of Ege,
Bornova,
35100 Izmir, Turkey

K. Ertekin (✉)
Dokuz Eylul Universitesi Fen-Edebiyat Fakultesi Kimya Bolumu,
Tinaztepe Buca,
35160 Izmir, Turkey
e-mail: kadriye.ertekin@deu.edu.tr

Introduction

Ruthenium complexes have been extensively synthesized and studied for many potential applications such as optical sensors, solar energy conversion systems, electronic devices and chemical/electrochemical catalysis [1–3]. They have been designed with specific ligands (e.g. hydride, halide, hydrate, carboxylate, phosphane, amine, oxygen or nitrogen chelating groups, Schiff bases, arenes, carbenes, etc.). As a result of the variety of ligands, ruthenium complexes exhibit different activity, selectivity and functionality in organic transformations and changing response to oxygen and moisture [4–8].

Ruthenium (II) complexes have also been widely used as oxygen indicators due to their efficient luminescent properties, relatively long-life metal-to-ligand charge transfer excited states, fast response times, strong visible absorptions, large Stoke's shifts and high photochemical stabilities [9–13].

In this work, three newly synthesized ruthenium complexes (Fig. 1) were characterized, their photophysical constants were calculated and utility of complex (I) was investigated in non-aqueous media in presence of nonadecafluorodecanoic acid as oxygen sensing material.

In recent applications the ruthenium based sensor signal has been enhanced by employing fluorine-containing polymers into the experimental media [13–18]. Promising studies with fluorine containing polymers encouraged us to use the clinically important perfluoro compounds as oxygen carriers in solution phase. Perfluorochemicals (PFCs) are non-polar highly fluorinated compounds and as a result of their strong intra-molecular C–F bonds, they are chemically and biochemically inert [19–21]. They have a high solubility for oxygen; which is about 20 to 30 fold than that of the oxygen solubility in plasma or water. However, most of the PFCs are not miscible with plasma or water, which looks like a problem in clinical studies [19–23]. Here

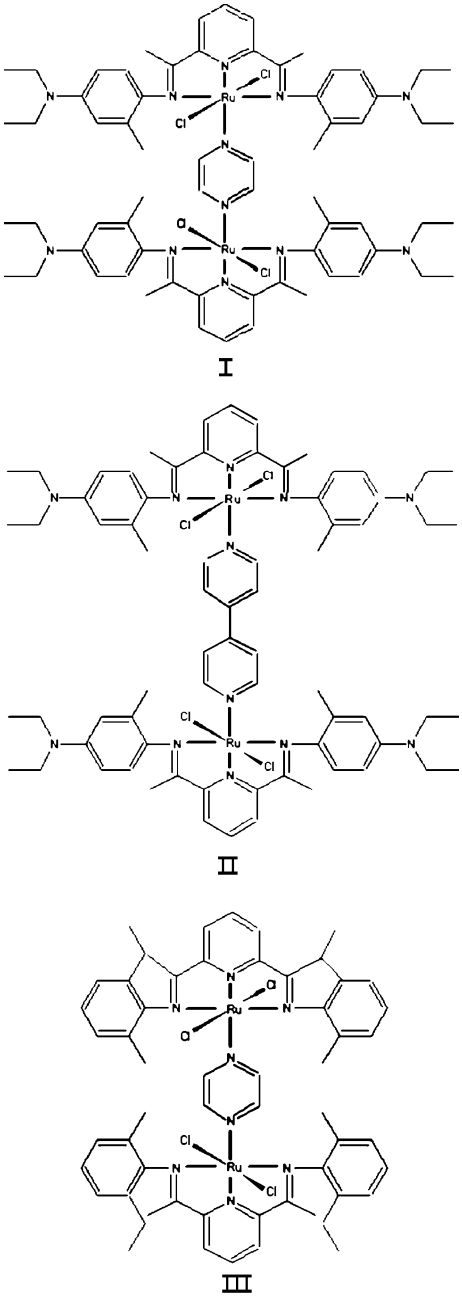

Fig. 1 Chemical structures of the ruthenium dyes of I, II and III

we used the solubility advantage of PFCs in non-aqueous ethyl alcohol and evaluated the response of ruthenium complex (I) to the oxygen in presence of perfluoro compound; nonadecafluorodecanoic acid.

Experimental

Materials and equipment

All of the solvents and chemicals used were analytical grade and purchased from Merck, Johnson and Mathey, Acros, Alfaaeser, Fluka and Riedel. Solvents for the spectroscopic studies were used without further purification. The PFC [nonadecafluorodecanoic acid; $CF_3(CF_2)_8CO_2H$] and quinine sulphate were purchased from Fluka. Ruthenium complexes of {(μ-pyrazine)bis-[{2,6-bis[1-(2-methyl-4-*N*,*N*-diethylaminophenylimino) ethyl]pyridine}dicholorodiruthenium(II)]}, (I), {(μ-4,4′-bipyridine)bis-[{2,6-bis[1-(2-methyl-4-*N*,*N*-diethylamino-phenylimino)ethyl]pyridine}dicholorodiruthenium(II)]} (II) and {(μ-pyrazine)bis-[{2,6-bis[1-(2-methyl-6-ethylphenylimino)ethyl]pyridine}dicholorodiruthenium (II)]} (III) were synthesized according to the published procedure [24, 25].

Absorption spectra were recorded using a Shimadzu UV-1601 UV-visible spectrophotometer. Steady state fluorescence and excitation spectra were measured using Varian Cary Eclipse Spectrofluorometer with a Xenon flash lamp as the light source. The excitation and emission slits were set to 5 nm during the investigation of photo-luminescent properties and 10 nm for oxygen sensing studies. The detector voltage was 600 V. Oxygen and nitrogen gas cylinders were of 99.9% purity and obtained from Gunes Company, Izmir, Turkey.

UV-Vis absorption-fluorescence emission based studies

The absorption, excitation and corrected emission spectra of the ruthenium complexes were recorded in aprotic solvents of DCM and THF, and in protic solvent of EtOH. As explained by Velapoldi et. al., the response function of the detection system can be calibrated by using a standard lamp and a diffuser in the sample position [26]. To acquire the corrected emission spectra, the diffuser (commercially available diffuser of spectrofluorometer) with a reflecting surface of 45° was located into the sample compartment. The Stoke's shift values, molar extinction coefficients and quantum yields were extracted from the spectral data (see Figs. 2 and 3). In order to obtain the excitation spectra, the Ruthenium complexes I, II and III were monitored at their maximum emission wavelengths; 400, 407 and 340 nm, respectively (see Fig. 3).

Fluorescence quantum yield calculations

Fluorescence quantum yield values (ϕ_F) of the ruthenium complexes were calculated employing the comparative William's method [27], which involves the use of well-characterized standards with known ϕ_F values. For this purpose, the UV-Vis absorbance and corrected emission spectra of five different concentrations of reference standards (quinine sulphate; Fluka AG 22640, >99%, ϕ_F=0.54) and ruthenium complexes were recorded. Quinine sulphate has been used in 0.05 M sulphuric acid.

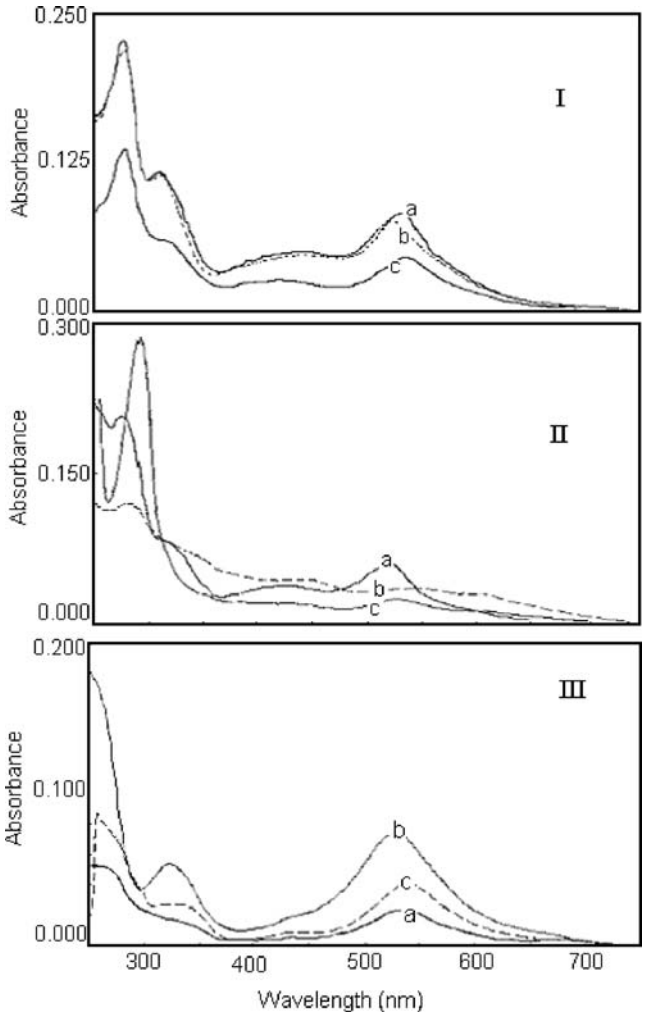

Fig. 2 Absorption spectra of the ruthenium complexes of I, II and III in the solvents of *a* DCM, *b* EtOH, *c* THF

The integrated fluorescence intensities of the ruthenium complexes were plotted vs absorbance values (Fig. 4). The gradients of the plots are proportional to the quantity of the quantum yield of the studied molecules.

The linearized calibration plots of ruthenium complexes I, II and III can be described by the equations and the relevant correlation coefficients of [$y=4.2951x$, $R^2=0.9922$]; [$y=3.9907x$, $R^2=0.9946$] and [$y=3.5458x$, $R^2=0.9966$], respectively. For the quantum yield standard, calibration plot equation and regression coefficients were [$y=1904.55x$] and $R^2=0.9981$, respectively.

Quantum yield (ϕ_F) values were calculated according to the following equation where ST and X denote standard and sample respectively, Grad is the gradient from the plot and n is the refractive index of the solvent [27].

$$\phi_X = \phi_{ST}\left(\frac{\mathrm{Grad}_X}{\mathrm{Grad}_{ST}}\right)\left(\frac{n_X^2}{n_{ST}^2}\right)$$

According to the data given in Table 1, all of the complexes exhibited moderate quantum yields ranging from 1.06×10^{-3} to 8.3×10^{-4}. Complex I was chosen for further studies due to the higher quantum yield and good solubility in EtOH and DCM.

Fluorescence decay time measurements

Fluorescence decay time of ruthenium complex (I) in DCM was determined with a lifetime apparatus equipped with a pulsed-nitrogen laser lamp in the laboratories of University of Perpignan, France. The apparatus was already described elsewhere [28]. A nitrogen laser (LSI VSL 337 ND) delivers monochromatic pulses at a wavelength of 337 nm

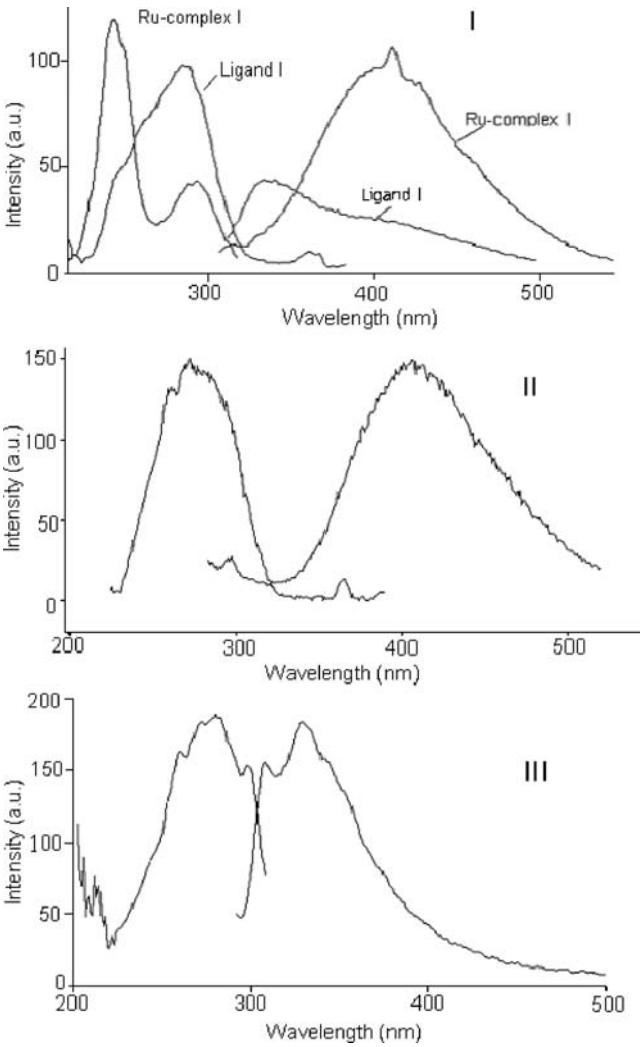

Fig. 3 *I* Gathered emission and excitation spectra of ruthenium complex I and ligand-1 (λ_{ex}=310 nm, λ_{em}=400 nm for ruthenium complex I; λ_{ex}=292 nm, λ_{em}=334 nm for L-1); *II* excitation and emission spectra of ruthenium complex II (λ_{ex}=290 nm, λ_{em}=407 nm); *III* excitation and emission spectra of ruthenium complex III (λ_{ex}=280 nm, λ_{em}=340 nm) in DCM

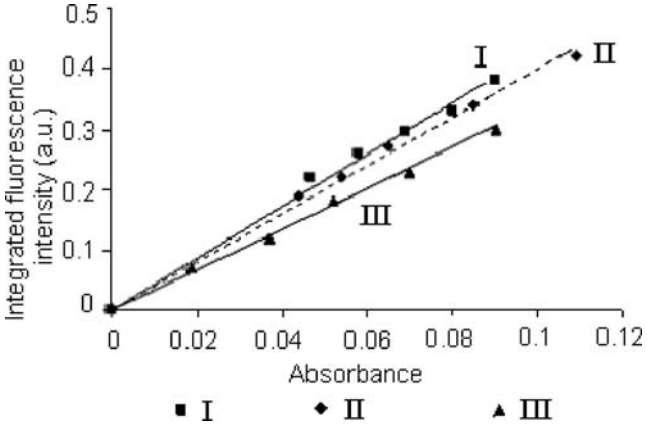

Fig. 4 The integrated fluorescence intensities vs absorbance values of the ruthenium complexes I, II and III. The gradients of the plots are proportional to quantum yields

with a half-amplitude pulse width of 3 ns. A 404-nm bandpass filter (half bandwith 40 nm) is placed in the emission path to select the ruthenium emission. Response of the apparatus can be simulated with a Gaussian curve convoluted with a time constant. The parameters of the Gaussian curve and the time constant were calibrated with a solution of 1,4-di-[2-(5-phenyloxazolyl)]-benzene. The employed molecule exhibited single-exponential decay. The decay time of 226 ns proves that reported emission originates from the ruthenium complex. This result is in accordance with the literature information acquired for the ruthenium complexes of $[Ru(bpy)_3]^{2+}$, $[Ru(phen)_3]^{2+}$ and $[Ru(dpp)_3]^{2+}$ [29]. Figure 5 reveals the fluorescence decay profile of the ruthenium dye under ambient air in DCM. The peaks of noise on the residual curve can be attributed to the moderate quantum yield of the ruthenium complex (I) rather than ligand based impurity.

Results and discussion

Spectral data and photophysical constants

The ruthenium dyes (I, II and III) exhibited excellent photostabilities in all of the solvents employed. The absorption spectra of the complexes I–III recorded in the solvents of different dielectric constants (ranging from 24.3 to 7.52 Debye) are gathered in Fig. 2 (a, b and c). Spectral shapes of the three complexes in DCM exhibited similarities. Ruthenium complexes I and II exhibited intense ligand -centred absorption bands around 236–268 nm (λ^1_{abs}), and 278–314 nm (λ^2_{abs}), and, a broad absorption band between 536–566 nm (λ^4_{abs}) with different molar extinction coefficients (see Fig. 2, Table 1). The intensive absorption bands of the complexes I and II can be attributed to the electron donating property of the subsituent N,N-diethylamino (DEA). An interligand charge transfer (ILCT) process is believed to be involved from DEA moiety to the pyridinediimine. The strong electron donating property of the DEA subsituent in the complexes I and II rises the energy level of the DEA part and an energy transfer from DEA (π) to the pyridinediimine (π^*) occurs. The ligand centred absorption bands of complexes I and II in DCM around 260 nm have high molar extinction coefficients (ε_I= 61,000, ε_{II}=76,202). However, in the absence of DEA, the molar extinction coefficient of the same band of complex III dramatically decreases (16,000) which can be concluded as an evident of the above mentioned ILCT. There was little absorption beyond 600 nm in all of the solvents employed.

In order to clarify any uncertainities arising from ligand based interferences, we recorded overlapping UV-Vis spectra of ligands and metal complexes. The overlaying absorption spectra of the ruthenium complex-I and ligand-1 (L-1); ({(μ-pyrazine)bis-[{2,6-bis[1-(2-methyl-4-N,N-diethylaminophenylimino)ethyl]pyridine}dicholorodiruthenium(II)]}) in DCM has been shown in Fig. 6. The dark purple complexes and pale yellow or white ligand molecules exhibited different absorption spectra.

Molar extinction coefficients and maximum absorption wavelengths of the three novel ruthenium complexes in different solvents are given in Table 2.

The excitation and emission spectra of the complexes in DCM are shown in Fig. 3 (a, b and c) respectively.

The ruthenium complexes I, II and III were excited at 310, 290 and 280 nm and the emission spectral data were acquired as well shaped emission bands at maximum emission wavelengths of 400, 407 and 340 nm, respectively. In spite of their typical colors; which range from dark purple to pale black, employed ruthenium complexes exhibited atypical emission bands. It was impossible to excite the Ru(II) complexes at longer wavelengths. This can be attributed to the presence of the two "weak field" Cl ligands coordinated to each Ru(II) center.

In comparison with complex III, the emission spectra of I and II exhibited 60 and 67 nm blue shift because of the

Table 1 Fluorescence spectroscopy related data: excitation wavelength, λ_{ex}, maximum emission wavelength, λ_{em}, Stoke's shift, $\Delta\lambda_{ST}$ and quantum yield, θ_F of the ruthenium dyes I, II and III in DCM

Ruthenium dye	Solvent	λ_{ex} (excitation wavelength, nm)	λ_{em} (max. emission wavelength, nm)	$\Delta\lambda_{ST}$ (Stock's shift, nm)	θ_F (Quantum yield)
I	DCM	310	400	85	1.06×10^{-3}
II	DCM	290	407	101	9.7×10^{-4}
III	DCM	280	340	23	8.3×10^{-4}

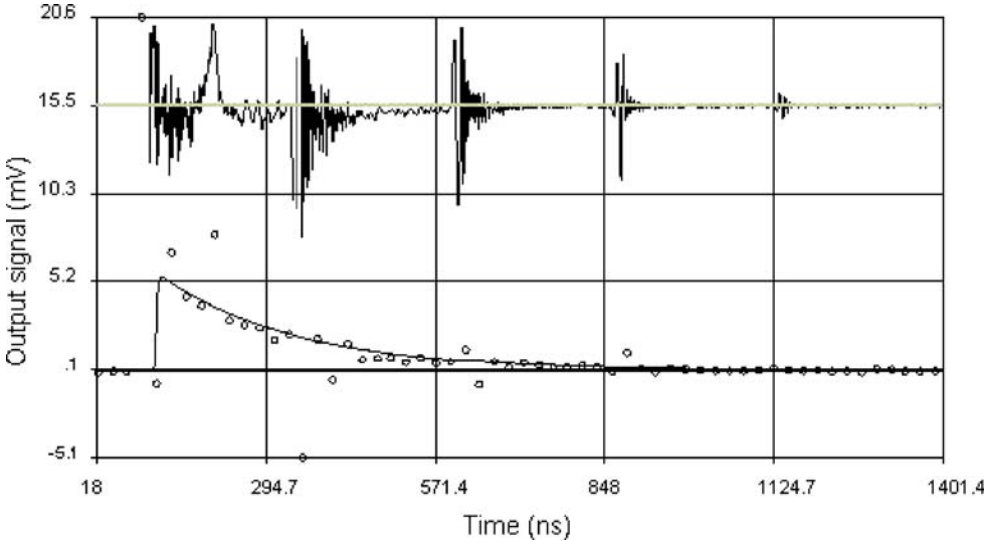

Fig. 5 Time resolved fluorescence decay profile of ruthenium complex (I) (10^{-6} M, in DCM). The *solid line* through the decay curve shows the calculated single exponential curve. The associated weighted residual curves are shown above the figures

longer π system conjugation and due to the presence of non paired "*n*" electrons of nitrogen atoms of diethyl amino groups (see Fig. 1).

The quantum yield values of the studied complexes are not as high as of the quantum yield values of red emitting Ru(N-N)2(4,4′-dicarboxylic 2,2 bipyridine and 4,4′-2,2′-bipyridine mono carboxy amide complexes [30], but approximately two or three times higher than the Ru(II) bis(2,2′:6′,2′-terpyridyl) complex [31]. Our values are in accordance with literature [31] and can be explained by electron delocalization approach. Extending the conjugation with bridging pyrazine (I and III) or 4,4′bipyridine (II) enhances the delocalization in dimer structures.

The Stoke's shift values in DCM were calculated from the spectral data and are 85, 101 and 23 nm for the Ru (II) complexes of I, II and III respectively (Table 1). Large Stoke's shift is desirable for fluorescence and solid state component containing optical sensor studies because the high Stoke's shift values allow the emitted fluorescence photons to be easily distinguished from the excitation photons, leading to the possibility of very low background signals.

Oxygen sensing studies

Oxygen sensing was carried out using different partial pressures of oxygen and nitrogen gases in the range of 0–

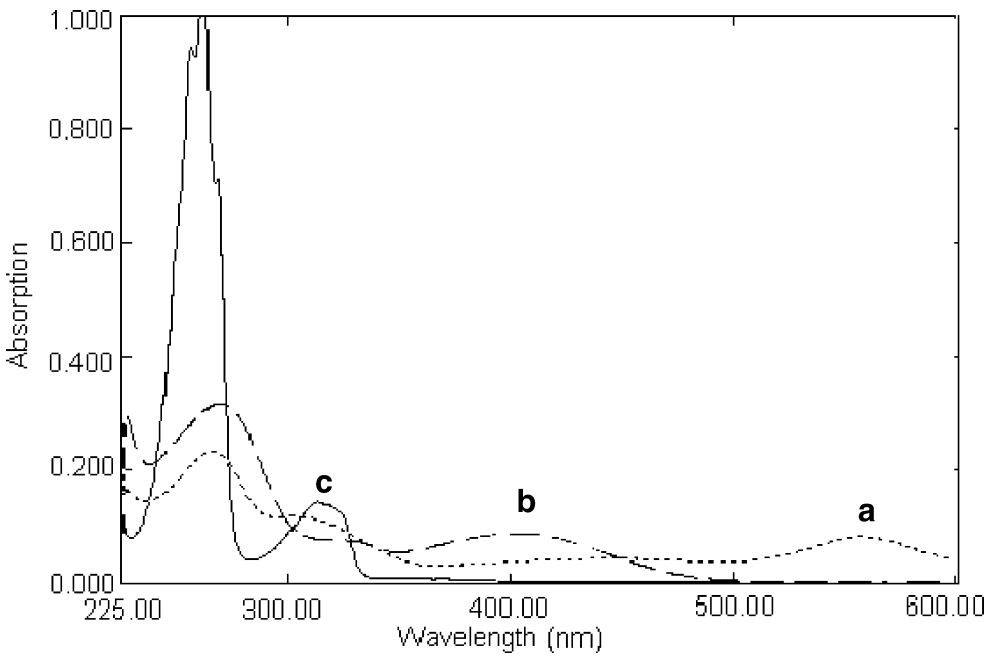

Fig. 6 The gathered absorption spectra of the ruthenium complex I (*a*), ligand-1 (*b*) and ligand-2 (*c*) in DCM

Table 2 UV-Vis spectroscopic data of the three ruthenium dyes in DCM, THF and EtOH

Ru Dye	Solvent	λ^1_{abs} (nm)	E (L/mol. cm) (molar extinction coefficient for λ^1_{abs})	λ^2_{abs} (nm)	λ^3_{abs} (nm)	λ^4_{abs} (nm)	E (L/mol. cm) (molar extinction coefficient for λ^4_{abs})
I	DCM	263	61,000	305	448	550	21,952
	EtOH	266	50,100	303	449	544	19,973
	THF	267	36,300	304	431	561	16,603
II	DCM	261	76,202	306	430	536	20,301
	EtOH	268	40,101	314	449	566	3,808
	THF	236	34,113	278	425	546	2,253
III	DCM	252	16,000	317	442	554	22,648
	EtOH	232	15,407	313	446	546	17,826
	THF	256	17,322	318	444	559	22,400

100% in a gas diluter (Sonimix 7000A gas blending system). The output flow rate of the gas mixture was maintained at 250 ml min^{-1}. Gas mixtures were introduced into the sensor agent-containing cuvette via a diffuser needle under ambient conditions.

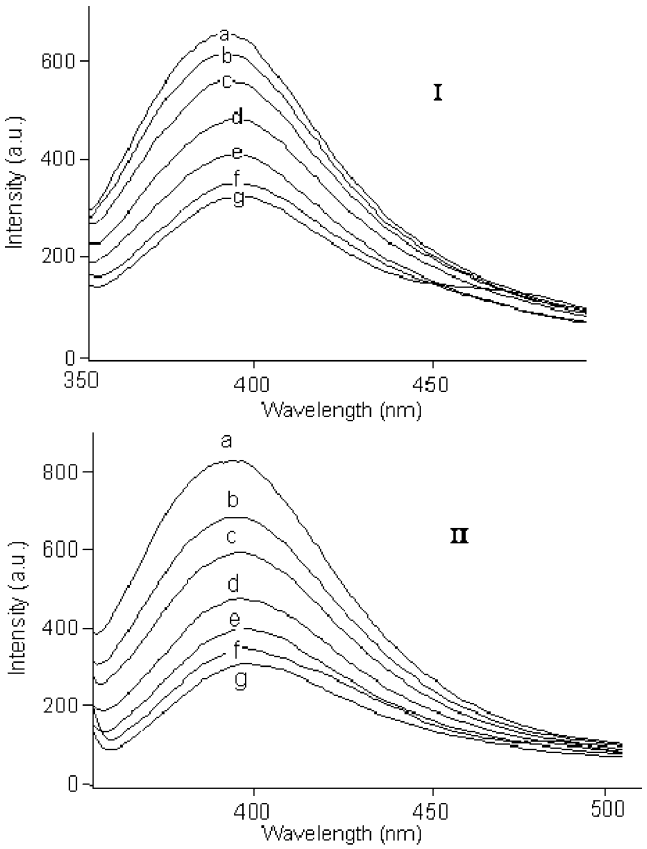

Fig. 7 Emission spectra of ruthenium complex-I after exposure to different partial pressures of oxygen gas. *I* In the absence, *II* in the presence of 3.24×10^{-3} M PFC in EtOH. *a* 0%, *b* 10, *c* 20, *d* 40, *e* 60, *f* 80 and *g* 100% oxygen

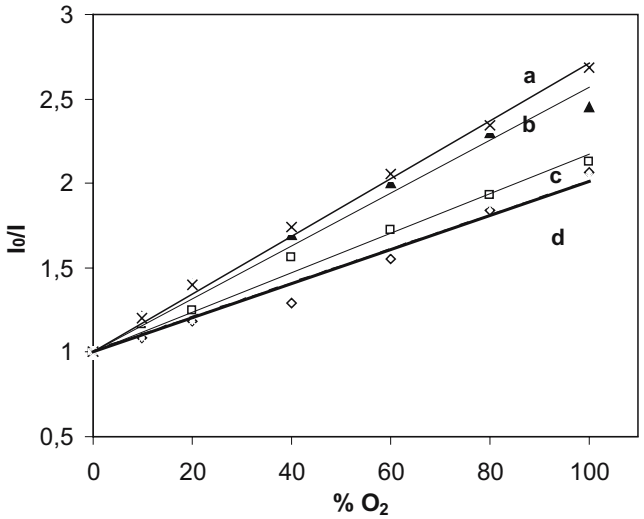

Fig. 8 Stern–Volmer plots for ruthenium complex-I in the presence of different concentrations of PFC. *a* 6.48×10^{-3} $M\times l^{-1}$, *b* 3.24×10^{-3} $M\times l^{-1}$, *c* 2.16×10^{-3} $M\times l^{-1}$, *d* 1.08 $M\times l^{-1}$ dissolved PFC in EtOH

The total output pressure of the gas mixture was maintained at 750 Torr. All of the experiments were carried out at room temperature of 25±1°C.

Complex I was chosen for the oxygen sensing studies because of its higher quantum yield, good solubility in EtOH, large Stoke's shift and longer excitation wavelength compared to the others. The oxygen sensitive composition yields a large absorption band ranging from UV to the initial of red light (Fig. 2, I). When excited at/310 nm, yields a broadened emission peak at λ_{max}=410 nm which responds to oxygen by a decrease in emission intensity that can be used as the analytical signal (Figs. 4, I and 6, I). Upon exposure to partial oxygen pressures from 0 to 100%, in the absence of PFC, sensing agent exhibits a 51% relative signal change in direction of decrease in fluorescence intensity.

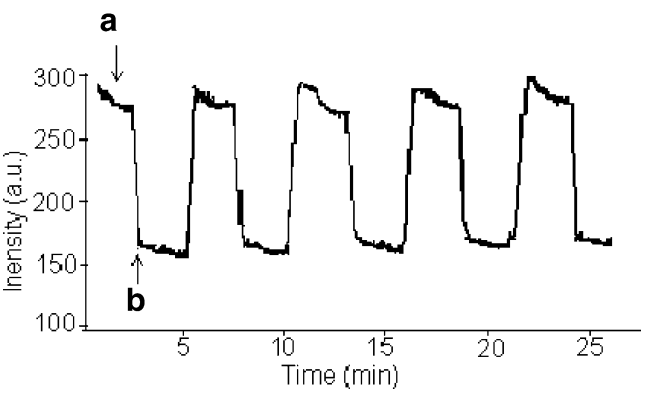

Fig. 9 Relative fluorescence intensity changes for ruthenium complex-I in the presence of 1 mM perfluorochemical on switching from *a* 100% nitrogen to 100% oxygen, *b* 100% oxygen to 100% nitrogen

On the other hand, PFCs are organic compounds in which all hydrogen atoms have replaced with fluorine atoms and therefore, they can dissolve large volumes of respiratory gases. Gas molecules occupy so-called 'molecular cavities' within liquid PFCs, but no chemical reactions are involved. This solubility is related to the molecular volume of the dissolving gas and is in the order of $CO_2 > O_2 > CO > N_2$ [21]. Therefore, a PFC added ethyl alcohol is expected to exhibit better oxygen solubility.

In our earlier experiments the solubility of oxygen and CO_2 has been increased by employing PFCs into the solid matrix materials, which resulted with an enhancement in the sensor performance [22, 23]. Interestingly, the ruthenium dye solution exhibited a higher and brighter fluorescence in presence of the fluorine rich PFC. It also exhibited a higher relative signal change value; 63% in direction of decrease in emission intensity, upon exposure to certain partial oxygen pressures from 0 to 100% in presence of $3.24\times10^{-3}\mathrm{M}\times\mathrm{l}^{-1}$ PFC in EtOH. This result reveals that a 23.6% enhancement has been observed in sensor performance in terms of relative signal intensity (see Fig. 7). In order to optimize the PFC concentration, four different concentrations of PFC has been tested.

The oxygen sensing properties of the sensing agent were characterized by I_0/I_{100} value and Stern–Volmer quenching constant. The Stern–Volmer plots are derived by using the below Stern–Volmer equation (Fig. 8)

$$I_0/I = K_{\mathrm{SV}\times}\mathrm{PO}_2 + 1$$

Where I_0 and I are the luminescence intensities in the absence and presence of oxygen, respectively. The plots were exhibited considerable linearity at oxygen concentrations in the range of 0–80%. Plot "a" can be described with the equation, $y = 0.0171x + 1$ and regression coefficient of R^2=0.9957. The Stern–Volmer constant (K_{SV}) was found to be 0.0171 (see Fig. 8). The plot of I_0/I vs partial pressure yields straight-line relationship with slope K_{SV}, and intercept at 1 on the y-axis. This result reveals the presence of a dynamic or diffusional quenching throughout the measurements in the solution phase. The I_0/I_{100} ratio was found to be 2.03 and 2.68 in absence and presence of PFC, respectively.

Figure 9 illustrates the response characteristics of the perfluorinated solution in an alternating atmosphere of 100% O_2 and 100% N_2. Response time is defined as the time taken to attain 90% of its original signal intensity (τ_{90}) when the gas is changed. In the presence of PFC, the response and recovery times for oxygen sensing after exposure to 100 and 0% O_2 were quite fast and found to be 20 s. In case of five replicate measurements, standard deviation of upper signal level was found to be 271.2±5.7.

Conclusions

In this study, photophysical characteristics of three novel ruthenium (II) complexes were declared; their structures were clarified and were investigated by means of spectroscopy in different solvents. The Stoke's shift values, quantum yields and molar extinction coefficients were extracted from spectral data. The Ruthenium complex (I), exhibiting the highest quantum yield has been used for oxygen sensing purpose. Solution of the ruthenium complex (I) exhibited a total relative signal change of 56% in direction of decrease in emission intensity upon exposure to partial oxygen pressures in the range of 0.0–100% pO_2 in presence of perfluoro chemicals. In this article, the usability of PFC's as oxygen carriers and sensor response enhancers in non-aqueous media is also proven.

Acknowledgements We thank Prof. Dr. Jean-Marie Salmon and Dr. Anne-Cecile Ribou for allowing time resolved based studies in their laboratory. Funding for this research was provided by the TUBITAK and Scientific Research Funds of Dokuz Eylul University (Project No.: 04.kb.fen.105).

References

1. Fraysse S, Coudret C (2000) Eur J Inorg Chem 7:1581
2. Hirao T, Iida, K (2001) J Chem Soc Chem Commun 431
3. Goulle V, Harriman A, Lehn JM (1993) J Chem Soc Chem Commun 1034
4. Clapham SE, Hadzovic A, Morris RH (2004) Coord Chem Rev 248:2201
5. Bianchini C, Casares JA, Peruzzini M, Romerosa A, Zanobini F (1996) J Am Chem Soc 118:4585
6. Miyata A, Furukawa M, Irie R, Katsuki T (2002) Tetrahedron Lett 43:3481
7. Shrikanth A, Nagendrappa G, Chandrasekaran S (2003) Tetrahedron 59:7761
8. Antonya R, Tembea GL, Ravindranathana M, Ramb RN (1998) Polymer 39:4327
9. Hu YZ, Tsukiji S, Shinkai S, Oishi S, Dürr H, Hamachi I (2000) Chem Lett 442
10. Hirao T, Fukuhara S (1998) J Org Chem 63:7534
11. Moriuchi T, Bandoh S, Miyaishi M, Hirao T (2001) Eur J Inorg Chem 651
12. Choi MF, Xiao D (2000) Anal Chim Acta 403:57
13. Fujiwara Y, Amao Y (2004) Sens Actuators B Chem 99(1):130
14. Amao Y, Tabuchi Y, Yamashita Y, Kimura K (2002) Eur Polym J 38(4):675
15. Amao Y, Asai K, Miyashita T, Okura I (2000) Polm Adv Technol 11:705
16. Amao Y, Miyashita T, Okura I (2001) J Porphyr Phathalocya 5:433
17. Amao Y, Miyashita T, Okura I (2001) J Fluorine Chem 107:101
18. Amao Y, Miyashita T, Okura I (2001) React Funct Polym 47:49
19. Riess J (2001) Chem Rev 101:2797
20. Dias AMA, Freire M, Coutinho JAP, Marrucho IM (2004) Fluid Phase Equilib 222(223):325

21. Lowe KC (2002) J Fluorine Chem 118(1–2):19
22. Ertekin K, Kocak S, Ozer MS, Aycan S, Cetinkaya B (2003) Talanta 61(4):573
23. Ertekin K, Alp S (2006) Sens Actuators B 115:672–677
24. Çetinkaya B, Çetinkaya E, Brookhart M, White PS (1999) J Mol Cat A Chem 142:101
25. Dayan O, Çetinkaya B (2007) J Mol Cat A Chem 271:134–141
26. Velapoldi H, Tonnesen H (2004) J fluoresc 14(4):465
27. Williams ATR, Winfield SA, Miller JN (1983) Analyst 108:1067
28. Ribou AC, Vigo J, Kohen E, Salmon JM (2003) J Photochem Photobiol B Biol 70:107
29. Mongey K, Vos JG, MacCraith BD, McDonagh CM (1997) J Sol-Gel Sci Technol 8:979–983
30. Shen Y, Maliwal BP, Lakowicz JR (2003) J fluoresc 13(2):163
31. Benniston AC, Chapman G, Harriman A, Mehrabi M, Sams CA (2004) Inorg Chem 43:4227